# INTERNATIONAL SOCIETY FOR SOIL MECHANICS AND GEOTECHNICAL ENGINEERING



This paper was downloaded from the Online Library of the International Society for Soil Mechanics and Geotechnical Engineering (ISSMGE). The library is available here:

https://www.issmge.org/publications/online-library

This is an open-access database that archives thousands of papers published under the Auspices of the ISSMGE and maintained by the Innovation and Development Committee of ISSMGE.

# Failure induced pore pressure, experimental results and analysis

Länsivaara, T., Lehtonen, V. & Mansikkamäki, J. Tampere University of Technology, Tampere, Finland



#### **ABSTRACT**

When soft clays are loaded, the loading itself generates an excess pore pressure build up. If one intends to do an undrained effective stress failure analysis, it is uttermost important to account for this pore pressure to receive a proper safety assessment. In analysis based on the limit equilibrium method (lem) this is often disregarded, while in finite element method (fem)analysis the amount of pore pressure build up may easily be underestimated due to use of false soil model or improper soil parameters.

To study this subject, a full scale failure test on an existing railway embankment on very soft and sensitive clay has been conducted. The loading was done by filling sand on reinforced shipping containers laid upon steel frameworks to simulate railway cars. The test area was instrumented extensively to get a proper picture of excess pore pressures and displacements during the loading and failure process.

# RÉSUMÉ

Lorsque les argiles mous sont chargés, le chargement génère un excès de pression interstitielle. Pour effectuer une analyse non drainée effective de rupture de contrainte, il est impératif de tenir compte de cette pression de pore dans le but d'obtenir une évaluation de sécurité adéquate. Dans l'analyse fondée sur la méthode d'équilibre limite (LEM) cet aspect est souvent négligé, alors que dans la méthode des éléments finis (FEM) l'analyse de la quantité de pression interstitielle produite peut être facilement sous-estimée en raison de l'utilisation d'un modèle de sol inadéquat ou de paramètres du sol incorrects.

Pour étudier ce sujet, un test grandeur nature sur un remblai de chemin de fer existant sur une terre battue très douce et sensible a été réalisé. Le chargement a été effectué en remplissant de sable des containers d'expédition maritime renforcés placés sur des cadres en acier afin de simuler des wagons de chemin de fer. La zone d'essai a été soumise à une instrumention intensive pour obtenir une image correcte de l'excédent des pressions interstitielles et des déplacements lors du chargement et du processus de rupture.

# 1 INTRODUCTION

Failure calculations for clays in undrained conditions are often done applying the rather simple concept of undrained shear strength. Although much used, it has its limitations and may for some cases lead to an under prediction of safety. An alternative is then to apply the effective stress strength parameters and do an undrained effective stress analysis. However, failures in soft clays are usually preceded by a build up of excess pore pressures. addition to loading or water/precipitation caused pore pressure, the vielding of the clay also induces additional pore pressures. If failure analysis like stability calculations are conducted using undrained effective stress analysis, it is thus most vital to account for both the initial pore pressure, and the excess pore pressures developed during the failure itself. In limit equilibrium analysis the failure or yield induced pore pressure is usually totally ignored causing an over prediction of safety.

A full scale failure load test on an existing railway embankment has been conducted to study the development of yield induced pore pressure and to develop effective stress based calculation methods for the problem.

# 2 FAILURE (YIELD) INDUCED PORE PRESSURE

When soft clays are loaded in undrained conditions, they tend to exhibit a pore pressure build up that might be higher than the actual load increase. Such excess pore pressures might also develop simply due to shear without any external load increase on the specific soil element. The explanation for such yield induced pore pressure can be given as follows.

A stress increase on a soft normally consolidated clay results in yielding, i.e. breakdown of the soil skeleton. This causes a tendency for large volumetric compression. However, due to the low permeability of the clay the water cannot dissipate, and an undrained condition with pore pressure build instead of volumetric compression is displayed. In terms of soil modeling, the tendency to large positive plastic volumetric straining needs to be compensated by negative elastic straining, which is possible only by a reduction in effective stresses.

It is also well known that creep or time effects play a significant role in soft clay behaviour. In oedometer testing higher loading rates results in higher stresses for the same amount of compression. This is shown e.g. in the rate dependency of the preconsolidation pressure. Same kind of behaviour is also known from triaxial testing. The higher strain rates are used, the higher shear stresses are obtained while the pore pressure development is decreasing, Figure 1.

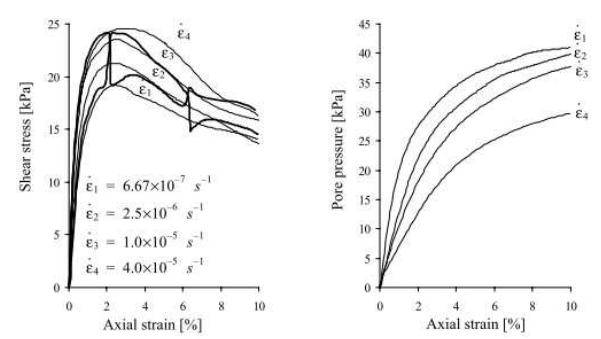


Figure 1. The effect of strain rate on undrained triaxial tests for four constant strain rate tests and two tests where the strain rate has been varied between the maximum and minimum values, Länsivaara (1999).

The phenomenon can be summarized as follows. The lower the loading rate is the more creep the clay exhibits. The volumetric compression is thus larger, which in undrained conditions leads to higher excess pore pressures. So in undrained testing of soil strength with triaxial apparatus, vane test or other method, low loading rate results in lower undrained shear strength, while higher loading rates give higher undrained shear strength. However, as shown by Janbu and Senneset (1995), the effective strength parameters are not influenced by loading rate, as the influence is on pore pressure.

A principal illustration of yield induced pore pressure for normally consolidated clay is shown in Figure 2. For low strain rates the stress paths follow quite closely the initial yield surface as large excess pore pressures are developed. For higher strain rates the stress paths are directed more upwards as less pore pressure is built up.

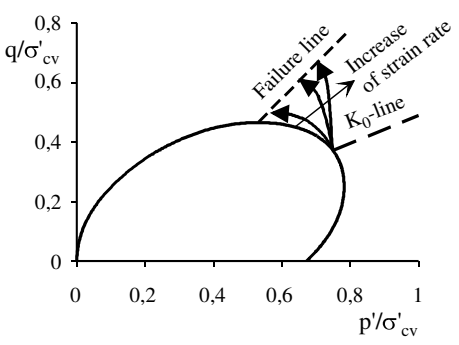


Figure 2. Principal sketch of undrained loading for normally consolidated clay, Länsivaara 2010.

# 3 FULL SCALE FAILURE LOAD TEST

Tampere University of Technology (TUT) and the Finnish Transport Agency conducted a full-scale railway embankment failure experiment in Salo, southern Finland. The purpose of the test was to get reliable data of pore pressure development in failure conditions. This knowledge will then further be used to develop calculations methods for stability. An additional goal for the experiment was to test the capability of different monitoring devised to act as warning systems for embankment failures.

#### 3.1 Soil conditions

The test site is located in Perniö, Salo right next to the coastal railway track between Helsinki and Turku. An old abandoned blind track that had been built in the 1960's where utilized as the actual test site. It is situated on the edge of a marine clay area. The upmost soil layer consists of the old embankment fill made of sand and gravel. Underneath a 1.0-1.5m thick layer of dry crust can be found, followed by a soft clay layer of 3 to 4m thickness. Under the clay layer a silty soil can be found followed by moraine. A typical cross section from the site can be found in Figure 3.

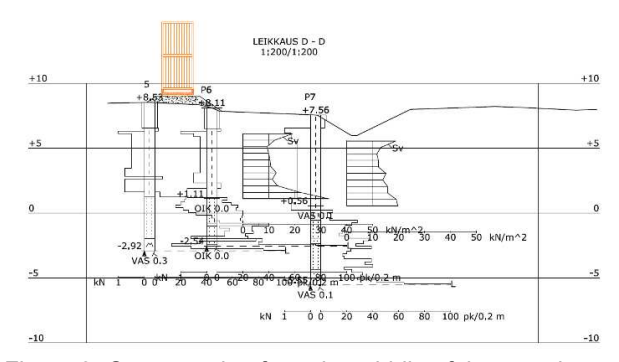


Figure 3. Cross section from the middle of the test site.

The clay is slightly overconsolidated and its undrained shear strength varies generally between 9 to 15 kPa increasing with depth. The water content of the clay varies in the range 70...90 % and the sensitivity of the clay is up to 40.

#### 3.2 Test layout

The old railway track consisted of light rails and wooden sleepers that were not considered to be sufficient for the failure load test. They were thus removed and a new, 0,55m high railway embankment with reinforced concrete sleepers and heavy rails was built on top of the existing one to a length of 60m.

Four steel frameworks, each 12m long, were placed on the tracks to simulate short rail cars with bogies. On top of each steel frameworks four modified sea containers were placed, two on top of each other. The containers were gradually filled with sand using a conveyor belt.

The test area was heavily instrumented with 37 straintype pore pressure transducers, 9 automatic inclinometer tubes (monitoring both transverse and longitudinal movement), 2 total stations monitoring a total of 27 prisms, 3 automatic settlement tubes (liquid filled flexible tubes that automatically and continuously measure settlement based on changes in hydrostatic pressure), 5 large earth pressure transducers installed lengthwise under the embankment, strain transducers for weighing the containers (the load was also controlled by weighing the loaded sand with a front loader), flexible vertical tubing for measuring the slip surface location and acceleration transducers for measuring the tilt angle of the containers. Altogether more than 300 measurement

points were continuously monitored on-line during the test.

Many variables (especially displacements) were measured with several different methods to ensure that enough reliable data would be obtained and to test the suitability of different methods for monitoring embankment stability. Pore pressure transducers were placed based on preliminary stability calculation to be sure that the yield induced pore pressure in the failure zone would be captured. The placement of key instruments is shown in Figure 4 and the placement of pore pressure transducers in the cross section in Figure 5

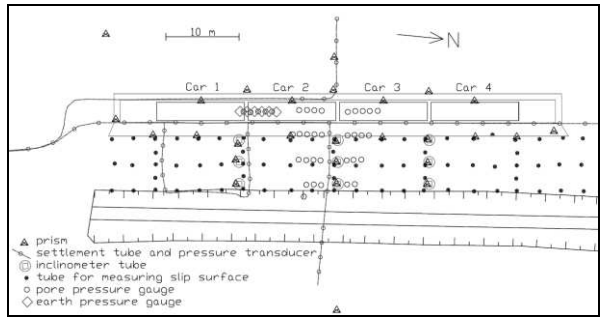


Figure 4. The placement of the main instrumentation (Lehtonen 2010).

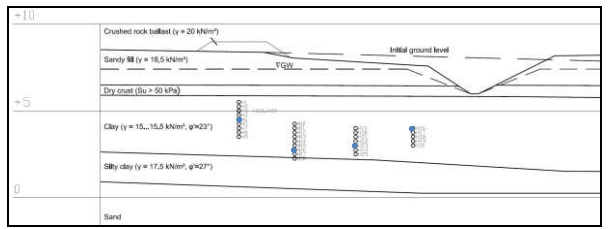


Figure 5. Location of the pore pressure transducers in relation to the cross section in the middle of the test site.

The loading was carried out during two days in October 2009. During the first day the two central "cars" were loaded with an equivalent of a 24 kPa homogenous train load (line load divided by the sleeper length of 2.5 m) and the outermost cars respectively to 20.5 kPa. This loading corresponds to a stress increases that brings the stress state close to the preconsolidation pressure.

On the second day the load was raised to maximum in 5 kPa steps for each car, each cycle taking about 45 minutes. The maximum load of 85...87 kPa was reached at 7:34 pm. The embankment collapsed two hours later at 9:27 pm, when cars 1, 2 and 3 quickly sunk and fell on their sides away from the ditch. Car number 4 fell a few seconds later almost directly to its side with very little settlement compared to the others. Significant ground movement could be seen, as the ground moved horizontally towards the ditch and bulged up between the embankment and the ditch.

A picture of the test site and the loading of the containers early on the second day is shown in Figure 6.



Figure 6. Test site and loading of the containers on the second loading day.

# 3.3 Results

True out almost the entire loading pore pressures and displacements developed quite linearly with respect to the applied loading. Herein focus will be put on the second day of loading, i.e. from 24 kPa onwards. In Figure 7 the excess pore pressure development for some of the transducers located closely to the final failure surface is presented with respect to time and loading. The behaviour is fairly linear during the whole loading process. After about half an hour after the loading stopped the pore pressures started rapidly to increase. The rapid increase started below the embankment while it took place somewhat delayed with increasing distance from the centerline of the embankment. This clearly demonstrates the progressive nature of the failure.

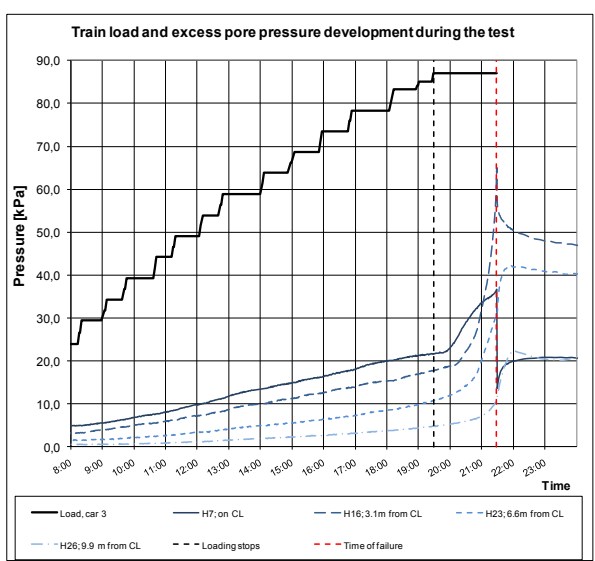


Figure 7. Excess pore pressure development for some selected points near the failure surface.

In Figure 8 excess pore pressure contours based on the measurements are presented in the middle sections of the failure test. Figure 8a) gives the excess pore pressures right after the full load have been reached,

while figure 8 b) represents the pore pressures nearly two hour later, 10 minutes before failure. Quite an extensive delayed excess pore pressure development can be seen from both Figure 7 and Figure 8.

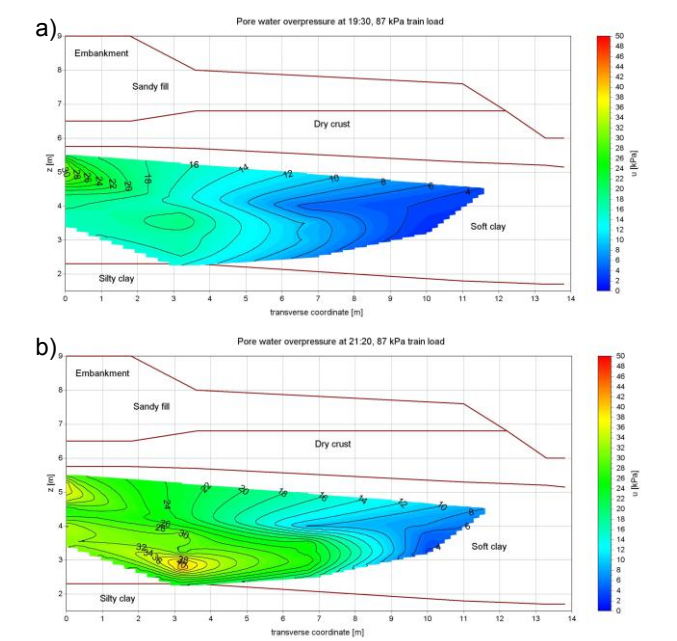


Figure 8. Excess pore pressure contours in the middle cross section of the failure test just after the loading ended a) and few minute before the failure b).

Three-dimensional geometry effects were significant in the failure progression. Although the actual failure occurred in seconds, certain phases can be distinguished. During the last 2-3 minutes before failure the rates and values of displacement (both vertical and horizontal movement) were largest near car no. 2. In the failure car 2 fell first, followed very closely by cars 1 and 3. Car 4 fell some seconds later with very little settlement compared to others. Measured horizontal displacements at ground surface towards the ditch after failure are presented in Figure 9.

The actual failure surface was approximately 30 to 40 m wide. While the distance from the embankment to the ditch was about 15m, it is obvious the 3D-effects were a significant factor that increased the initial resistance of the embankment against failure.

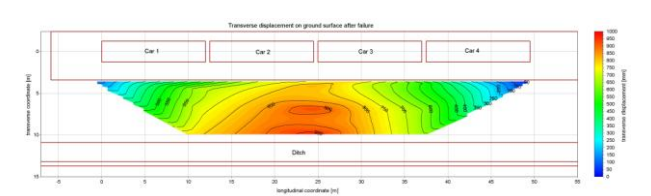


Figure 9. Measured horizontal displacements towards the ditch after failure.

#### 4 ANALYSIS

The failure test is used to develop both limit equilibrium (lem) and finite element methods. In this article the focus of analysis will be on lem analysis.

### 4.1 Yield induced pore pressure in lem

In limit equilibrium based stability analysis the stress conditions are described in a somewhat simplified way. Stress distribution is not considered, while stresses e.g. from external loads are transferred solely to the bottom of the slice upon which they act. Thus in undrained conditions one needs to compensate this stress increase by a pore pressure increase to avoid unrealistic increase of strength in undrained analysis with effective stresses.

All general methods assume an equal factor of safety along the slip surface and give an equilibrium strength/shear stress needed to balance the unstabilizing forces. Failure induced pore pressures are normally not accounted for. The equilibrium shear stress obtained from the analysis is therefore compared to a strength level corresponding to drained analysis, leading to an over prediction of strength and safety, see Figure 10

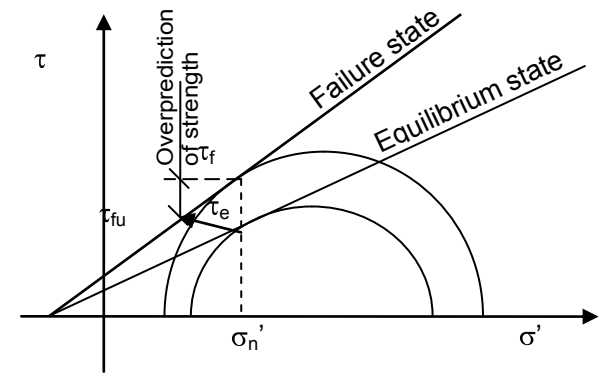


Figure 10. Overprediction of safety in conventional effective stress calculations for undrained conditions.

Failure induced pore pressure was introduce to lime equilibrium analysis at least already in 1981 by Svanö (Svanö 1981) with the undrained effective stress analysis or UESA concept. Herein a more simplified approach presented by Länsivaara (2010) is first presented. The main goal is to describe a method for accounting yield induced pore pressure for stability analysis of existing railway embankments of soft clays. In a later part further developments based on the UESA concept by Svanö are discussed.

The need for stability evaluations on the existing railway lines rises from the need to increase train loads. Therein the situation is that embankments have been built several decades ago on very soft clays. There might be some small overconsolidation in the clays due to aging effects, but under the embankments the clays are generally normally consolidated. If a failure state occurs, there will thus develop an excess pore pressure

corresponding to a stress change from the in situ state at  $K_{\mathit{ONC}}$  line to the failure state.

By assuming that the associated flow rule is valid for the  $K_0$  consolidation phase it is possible to determine the inclination of the initial (inclined) yield surface (Länsivaara 1995, Länsivaara 1999). The value for the  $K_{\text{ONC}}$  can quite accurately be determined from the friction angle using the Jáky equation. In Figure 11, some examples of estimations for yield surfaces using only the friction angle as input parameter is presented.

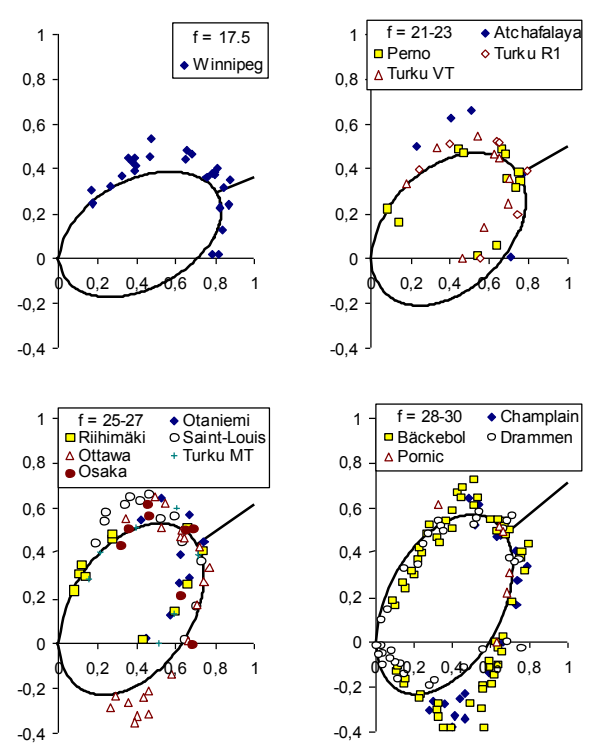


Figure 11. Yield surfaces classified by the friction angle and estimations made based on applying the associated flow rule at K<sub>oNC</sub> (Länsivaara 1999).

This can further be utilized to describe the difference in mean effective stress p' at  $K_0$  and the failure line (Länsivaara (2010). One can now describe both the initial hydrostatic stress  $p_{K0}$  and the failure hydrostatic stress  $p_f$  with the aid of preconsolidation pressure and friction angle, i.e.:

$$p_{ko} = f(\sigma_{cv}', \phi)$$
 [1]

$$p_f = f(\sigma_{cv}', \phi)$$
 [2]

Where  $\sigma_{cv}$ ' = preconsolidation pressure and  $\phi$  = friction angle. For a normally consolidated soil, the preconsolidation pressure can be substituted by the effective in situ vertical pressure. Estimation for failure induced pore pressure can then be obtained from Equation 3:

$$u_f = p_{kn} - p_f = f(\sigma_{kn}', \phi)$$
 [3]

In limit equilibrium method this can be used by applying a pore pressure parameter similar to  $r_u$ , with the exception that it now stands for failure induced pore pressure and should be applied to effective vertical stress. This pore pressure parameter is referred as  $r_u$  and is defined as:

$$r_{u}' = \frac{u_{ey}}{\sigma_{v0}'} = \frac{1}{\sigma_{v0}'} f(\sigma_{v0}', \phi)$$
 [4]

Where  $u_{ey}$  = yield induced excess pore pressure.

An equation for  $r_u$  can now be solved by using an inclined elliptical yield surface. For simplicity, the solution is herein presented in graphical form in Figure 12.

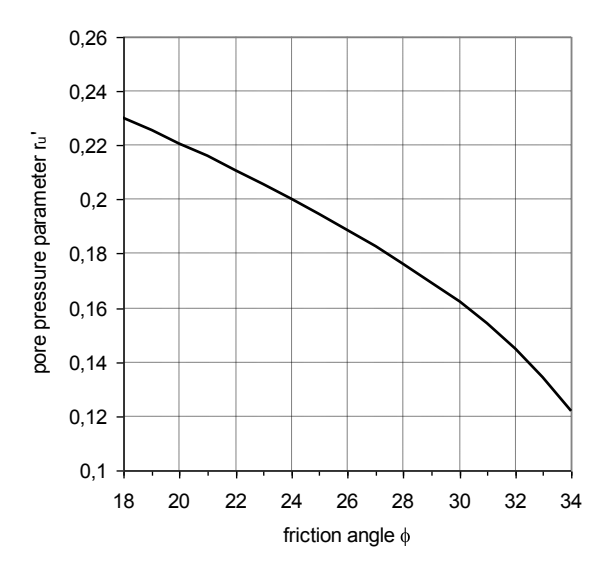


Figure 12. Effective stress pore pressure parameter  $r_u$ ' as function of friction angle (Länsivaara 2010).

As shown in Figure 12, the method gives a decreasing pore pressured development with increasing friction angle. The same phenomena can also be seen from the yield surfaces presented in Figure 11. With higher friction angles the yield surfaces are more inclined, and the relative horizontal distance from the  $K_0$ -line to failure on top of the yield surfaces decreases.

The procedure described above is strictly valid only for active (triaxial) case. So in limit equilibrium calculations, one should apply different solutions in shear and passive zones. Simply by looking at Figure 11, one might argue, that the failure induced pore pressure in the passive zone should be higher than in the active zone. However, as described earlier, the clays in southern Finland are often slightly overconsolidated due to aging. So while perfectly normally consolidated conditions usually occur under an existing embankment due its own loading, the clay next to the embankment in the passive zone is most likely slightly overconsolidated. Then, the development of excess pore

pressure due to failure in passive case is less than might be assumed by just looking at Figure 11. The intention herein is also to try and develop a simple way to account for failure induced pore pressure for engineering practice.

#### 4.2 Application to the failure load test

The effective pore pressure coefficient method has been applied for the Perniö failure load test. As has been discussed above, the actual failure load in the test was highly dependent on the loading rate/time. Had the applied load been slightly smaller, the failure had still occurred after a longer waiting time. The intention has not been, to include time effects in the limit equilibrium calculations. The calculated failure load should then correspond to the smallest failure load, corresponding to a long enough waiting time and corresponding excess pore pressure increase. As could be seen from Figure 9, the failure was three dimensional. The plane strain limit equilibrium calculations should thus give a lower bound value to the problem.

The calculation parameters for the different soil layers are presented in Table1.

Table 1. Soil parameter used in calculations

Soil layer	φ'	c'	γ
	0	kPa	kN/m3
Embankment	38	0	20
Sand Fill	36	0	19
Dry crust	0	30	17
Clay	24-25	0	15
Clayey Silt	27	0	16,5

In the analysis of such cases as this one, it is most important to use failure surfaces of arbitrary shape together with good search algorithms to find the most critical failure surface. In the present study modern optimization techniques introduce by Cheng (2003) and Cheng et al. (2008) are used in Novapoint Geoalc software. Compared to previous preliminary analysis (Länsivaara 2010) the implementation of the method has been improved and the soil layer geometry and values of soil parameters have become more precise with more laboratory testing.

The calculated failure loads are presented in Table 2 for both Janbu simplified and Morgenstern-Price methods using friction angles of 24° and 25° for the clay.

Table 2. Calculated failure load in kPa using Janbu simplified and Morgenstern-Price methods.

Friction angle for clay °	Janbu simplified kPa	Morgenstern- Price kPa
24	65	73
25	73	81

As discussed earlier the actual failure occurred with a load of 87 kPa on the two middle cars. As expected there is deviation between the methods and Janbu simplified gives a bit lower failure load. The sensitivity with respect to the friction angle gives also perspective that an accurate prediction of a single failure load value is rather illusive.

However, if no yield induced pore pressure would have been accounted for by the r<sub>u</sub>' method, the estimated failure load would have risen to 90 kPa with Janbu simplified method and 100 kPa with Morgenstern-Price method with a friction angle of 24°.

In addition to a slightly different failure load prediction, there is also a small difference in the location of the critical failure surface. Failure surfaces with Janbu simplified tend to go a bit deeper in the soft clay than with the Morgenstern-Price method. In this respect the failure surfaces with Janbu simplified corresponded quite accurately to the actual failure surface obtained from the tests. In Figure 13, all analysed failure surfaces with a factor of safety less than 1.05 are presented for Janbu simplified analysis using a friction angle of 24 degrees. Critical failure surfaces using Morgenstern-Price would approximately go near the upper level of the indicated range.

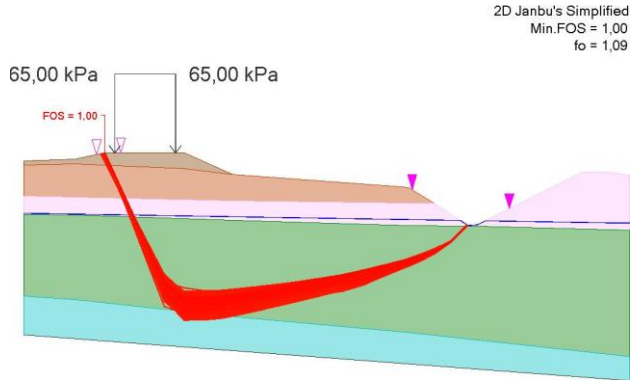


Figure 13. All analysed failure surfaces with a factor of safety below 1.05 for the Janbu simplified analyses using a friction angle of 24 degrees for the clay.

A simple way to account for the three dimensional nature of the failure surface in lem, is to calculate the end effects for the failure surface. As shown in Figure 9 the actual failure was far from ideal plane strain conditions. The primary failure developed in an area approximately 30 to 40 m wide. By accounting the end effects for a failure 30 m wide results in a failure load of 75 kPa with Janbu simplified method and 83 kPa with Morgenstern-Price method, both again assuming a friction angle on 24°. So in this case, the 3D nature of the failure surface increased the calculated capacity around 14-15%.

The excess pore pressures applied in the calculations are shown for two cases in Figure 14. The first case corresponds to the case in Figure 3, with a 65 kPa failure load for Janbu simplified and a friction angle of 24 degrees. The seconds was corresponds to a failure load of 84 kPa using also Janbu simplified but by accounting for the end effects and using a friction angle of 25

degrees. As can be seen, the difference is only under the train load, while the yield induced pore pressure in the shear and passive zones are similar for the two (alike) failure surfaces/cases.

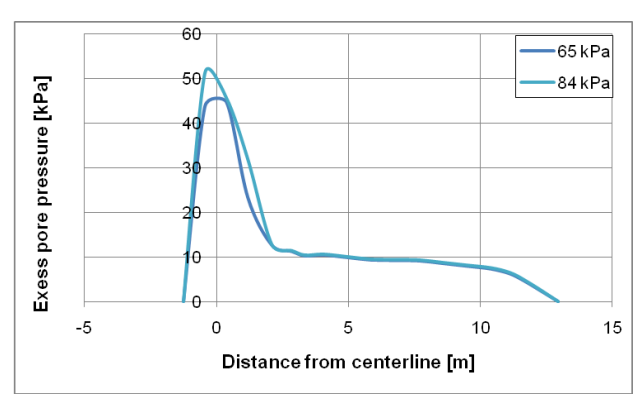


Figure 14. Excess pore pressure for two cases of Janbu simplified analysis.

Limit equilibrium calculations do not give a correct stress distribution in the soil. This is especially true for cases with high external loads. However, by comparing Figures 8 and 14, one can say, that the method gives quite a good and representative description of the yield induced pore pressures in the shear and passive zones.

#### 4.3 Further developments

In addition to the r<sub>u</sub>' calculation method, the concept of UESA by Svanö (1981) will further be developed in the present research project. In short, the original UESA concept included the calculation of an initial stress state and the calculation of a stress change due to load increase. The calculated stress change is then further utilized to calculate changes in pore pressure by a pore pressure parameter D. The calculation includes thus the excess pore pressure from the load change, but the factor of safety is still estimated as shown in Figure 10, i.e. the final failure/yield induced pore pressure is not accounted for. This will now be modified so, that instead of a excess pore pressure corresponding to the mobilized stress state, a pore pressure corresponding to the undrained failure stress state will be used.

As already discussed, applying the failure state pore pressure instead of the mobilized pore pressure arguably gives a better description of the true factor of safety regardless of the degree of mobilisation. The use of failure state pore pressure in the mobilized equilibrium state actually changes the analysis more towards the  $\phi$  = 0 calculations, where the mobilised shear stress is compared to the undrained shear strength that presumably represents the actual strength at failure.

An example of typical  $\sigma'$  –  $\tau$  stress paths using either mobilised or failure pore pressure is given in Figure 15. The consistent use of failure pore pressure results in a vertical stress path.

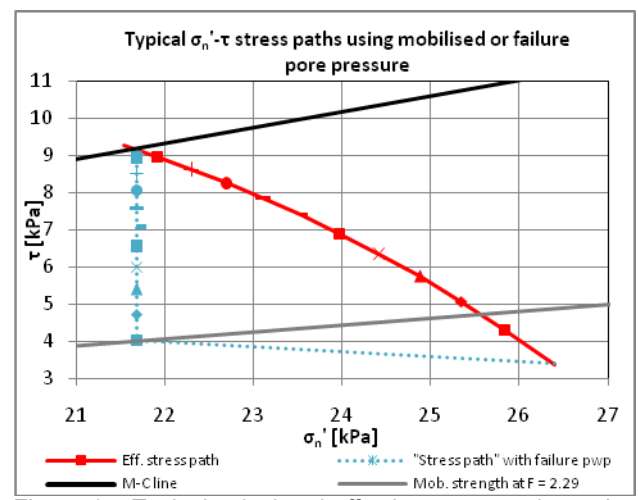


Figure 15. Typical calculated effective stress paths under an embankment subjected to an external load. Using failure pore pressure results in a vertical stress path. Similar markers denote similar external load levels. The stress paths coincide at F = 1.

It should be noted that the use of failure state pore pressure in the mobilised state does cause an error in the calculated mobilised shear stress, as the calculated normal stress acting on the bottom of the slice is much lower than when using mobilised ("true") pore pressure. This error in shear stresses is however much smaller (close to negligible) than the error that is otherwise made in calculating shear strength. Since LEM is generally not really used for calculating stresses anyway, this can be considered an acceptable trade-off considering the more accurate FOS.

The modified UESA concept is actually principally quite close to the  $r_{\rm u}$ ' method. However, it gives more freedom to account for various stress conditions and changes in the soil. Factors such as overconsolidation and principal stress rotation can more easily be taken into account. Assuming an anisotropic (rotated) yield surface defined by friction angle and preconsolidation pressure, the excess pore pressure can be fairly accurately calculated for any corresponding change in stress state. The limitations of the method are partly caused by those of the limit equilibrium methods themselves, as the calculations of stress conditions is not always that accurate, especially for cases with high external loads.

As already has been discussed, the time or the loading rate played a significant role in the performed failure test. Had the loading been ended somewhat earlier, it had still failed given enough time. It is probably not wise to try and introduce time effects in limit equilibrium calculations, while they should represent a safe estimate of failure load/safety factor. Time effects can be introduced in finite element calculations using hardening plasticity creep models. This is subject will be discussed in detail elsewhere with respect to Perniö failure load test. However, to give some indication of present estimation of time effects to the performed test, calculated failure loads for different loading rates are given in Figure 16. The calculations have been done using EVP-SCLAY1S-model (Karstunen & Yin 2010).

Accordingly there would be still quite a significant influence of time between loading time 4 and 14 day while at least after 14 days the influence can be neglected (not shown in the figure). It is of course difficult to say, how well the model captures the true magnitude of time dependency although the creep parameters used are determined by laboratory tests. The results are still preliminary, but will be further improved in coming studies.

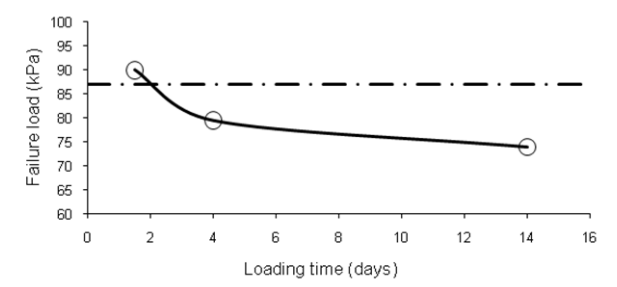


Figure 16. Preliminary fem calculations with creep for attempting to evaluate the influence of time to failure load.

#### 5 CONCLUSION

A full scale failure load test was performed on an existing railway embankment on soft clay. The test site was heavily instrumented with pore pressure gauges, displacement sensors and various other instruments with a total of more than 300 real time measurement points continuously followed.

The instrumentation worked well and a quite comprehensive picture of pore pressure and displacement development during the test was obtained. This data is used to develop both lem and fem stability calculation methods for undrained conditions. In addition, the data is used to evaluate the capability of different instruments to act as warning systems for low stability railway embankments.

In this article calculations based on the  $r_u$ '-method (Länsivaara 2010) has been presented. This method gives a rather simple way to account for yield induced pore pressure in the effective stress stability calculations for soft clays. If the yield induced pore pressures are neglected, the factor of safety is overestimed considerably.

# **ACKNOWLEDGEMENTS**

The writers would like to acknowledge the support from the Finnish Transport Agency in funding the project.

Also the contribution of Kauko Sahi, Heikki Luomala Marko Happo and Anssi Laaksonen in performing the failure load test is highly appreciated.

#### **REFERENCES**

- Cheng Y.M. (2003), Locations of Critical Failure Surface and some Further Studies on Slope Stability Analysis, Computers and Geotechnics, 30:255-267.
- Cheng, Y.M. Li, L., Länsivaara, T., Chib, S. C. and Sun Y.J. (2008). An improved harmony search minimization algorithm using different slip surface generation methods for slope stability analysis. Engineering Optimization.Vol. 40, No. 2, February 2008.
- Janbu, N., & Senneset, K. 1995. Soil parameters determined by triaxial testing. Proceedings of the 11th European Confer-ence on Soil Mechanics and Foundation Engineering, Copenhagen. Vol. 3 pp. 101-106
- Karstunen M.: Yin Z.-Y. (2010). Modelling time-dependent behaviour of Murro test embankment. Geotechnique vol.60.
- Lehtonen, V. (2010). Instrumentation and analysis of a full-scale embankment failure experiment. In: Bostik, J & Glisnikova, V. (Eds.) Geotechnical Engineering 20. View of Young European Geotechnical Engineers, Brno University of Technology, pp. 224–229. Conference proceedings, 20th EYGEC, Brno.
- Länsivaara, T. (1995). A critical state model for anisotropic soft soils. Proceedings of the 11th European Conference on Soil Mechanics and Foundation Engineering, ECSMFE, Vol. 6, Copenhagen.
- Länsivaara, T. 1999. A study of the mechanical behavior of soft clay. Doctoral dissertation. Norwegian University of Science and technology. Trondheim.
- Länsivaara, T. 2010. Failure induced pore pressure by simple procedure in LEM. In: Benz, T. et al. (eds.). Numerical Methods in Geotechnical Engineering. Proceedings of the Seventh European Conference on Numerical Methods in Geotechnical Engineering Numge 2010, Trondheim, Norway, 2-4 June, 2010 pp. 509-514.